Mesenchymal stem cells ameliorate renal fibrosis by galectin-3/Akt/GSK3β/Snail signaling pathway in adenine-induced nephropathy rat

Bo Chen, MD PhD, Southwest Medical University, China

Abstract (300 word limit)

Background: Tubulointerstitial fibrosis (TIF) is one of the main pathological features of various progressive renal damages and chronic kidney diseases. Mesenchymal stromal cells (MSCs) have been verified with significant improvement in the therapy of fibrosis diseases, but the mechanism is still unclear. We attempted to explore the new mechanism and therapeutic target of MSCs against renal fibrosis based on renal proteomics. **Methods**: TIF model was induced by adenine gavage. Bone marrow-derived MSCs was injected by tail vein after modeling. Renal function and fibrosis related parameters were assessed by Masson, Sirius red, immunohistochemistry, and western blot. Renal proteomics was analyzed using iTRAQ-based mass spectrometry. Further possible mechanism was explored by transfected galectin-3 gene for knockdown (Gal-3 KD) and overexpression (Gal-3 OE) in HK-2 cells with lentiviral vector. **Results**: MSCs treatment clearly decreased the expression of α-SMA, collagen type I, II, III, TGF-β1, Kim-1, p-Smad2/3, IL-6, IL-1β, and TNFα compared with model rats, while p38 MAPK increased. Proteomics showed that only 40 proteins exhibited significant differences (30 upregulated, 10 downregulated) compared MSCs group with the model group. Galectin-3 was downregulated significantly in renal tissues and TGF-β1-induced rat tubular epithelial cells and interstitial fibroblasts, consistent with the iTRAQ results. Gal-3 KD notably inhibited the expression of p-Akt, p-GSK3β and snail in TGF-β1-induced HK-2 cells fibrosis. On the contrary, Gal-3 OE obviously increased the expression of p-Akt, p-GSK3β and snail. **Conclusion**: The mechanism of MSCs anti-renal fibrosis was probably mediated by galectin-3/Akt/GSK3β/Snail signaling pathway. Galectin-3 may be a valuable target for treating renal fibrosis.

Keywords: Adenine, Mesenchymal stem cells, Interstitial fibrosis, Galectin-3, Proteomics

Image

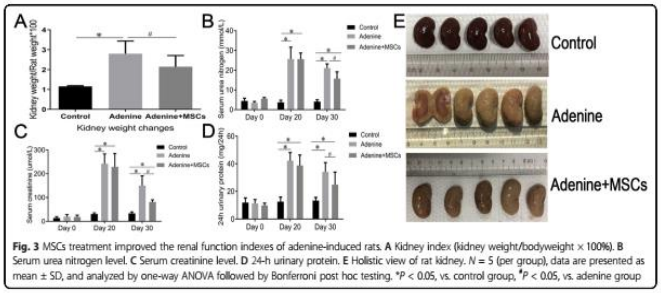

Fig. 3 MSCs treatment improved the renal function indexes of adenine-induced rats. **A** Kidney index (kidney weight/bodyweight × 100%). **B** Serum urea nitrogen level. **C** Serum creatinine level. **D** 24-h urinary protein. **E** Holistic view of rat kidney. $N = 5$ (per group), data are presented as mean ± SD, and analyzed by one-way ANOVA followed by Bonferroni post hoc testing. $^{*}P < 0.05$, vs. control group, $^{\#}P < 0.05$, vs. adenine group

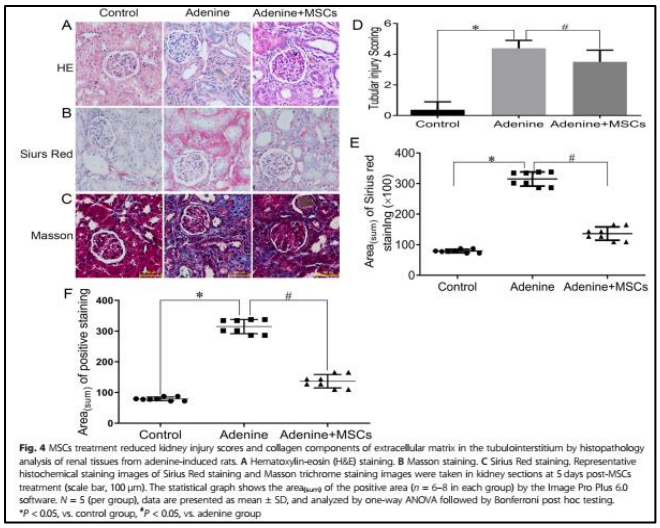

Fig. 4 MSCs treatment reduced kidney injury scores and collagen components of extracellular matrix in the tubulointerstitium by histopathology analysis of renal tissues from adenine-induced rats. **A** Hematoxylin-eosin (H&E) staining. **B** Masson staining. **C** Sirius Red staining. Representative histochemical staining images of Sirius Red staining and Masson trichrome staining images were taken in kidney sections at 5 days post-MSCs treatment (scale bar, 100 μm). The statistical graph shows the $area_{(sum)}$ of the positive area (n = 6–8 in each group) by the Image Pro Plus 6.0 software. $N = 5$ (per group), data are presented as mean ± SD, and analyzed by one-way ANOVA followed by Bonferroni post hoc testing. $^{*}P < 0.05$, vs. control group, $^{\#}P < 0.05$, vs. adenine group

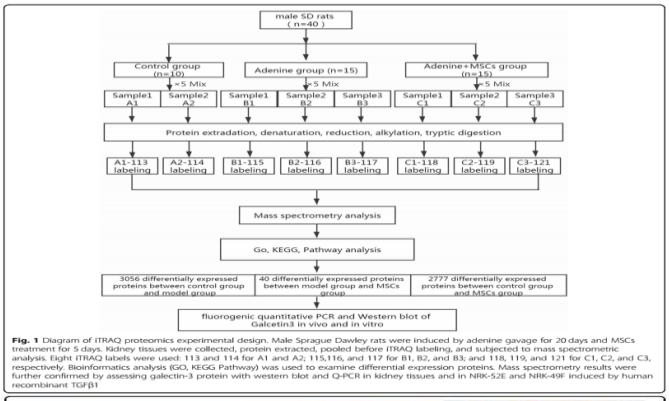

Fig. 1 Diagram of iTRAQ proteomics experimental design. Male Sprague Dawley rats were induced by adenine gavage for 20 days and MSCs treatment for 5 days. Kidney tissues were collected, protein extracted, pooled before iTRAQ labeling, and subjected to mass spectrometric analysis. Eight iTRAQ labels were used: 113 and 114 for A1 and A2; 115,116, and 117 for B1, B2, and B3; and 118, 119, and 121 for C1, C2, and C3, respectively. Bioinformatics analysis (GO, KEGG Pathway) was used to examine differential expression proteins. Mass spectrometry results were further confirmed by assessing galectin-3 protein with western blot and Q-PCR in kidney tissues and in NRK-52E and NRK-49F induced by human recombinant TGFβ1

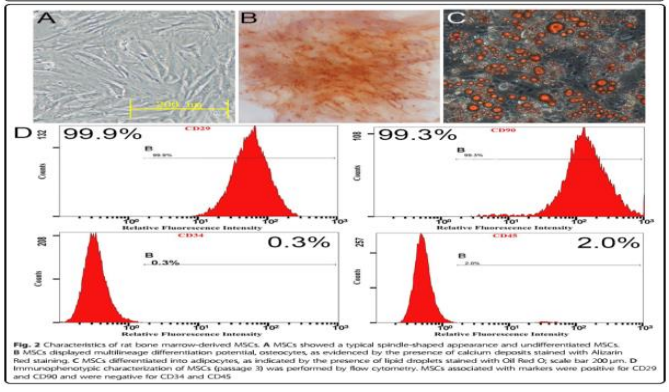

Fig. 2 Characteristics of rat bone marrow-derived MSCs. **A** MSCs showed a typical spindle-shaped appearance and undifferentiated MSCs. **B** MSCs displayed multilineage differentiation potential, osteocytes, as evidenced by the presence of calcium deposits stained with Alizarin Red staining. **C** MSCs differentiated into adipocytes, as indicated by the presence of lipid droplets stained with Oil Red O; scale bar 200 μm. **D** Immunophenotypic characterization of MSCs (passage 3) was performed by flow cytometry. MSCs associated with markers were positive for CD29 and CD90 and were negative for CD34 and CD45

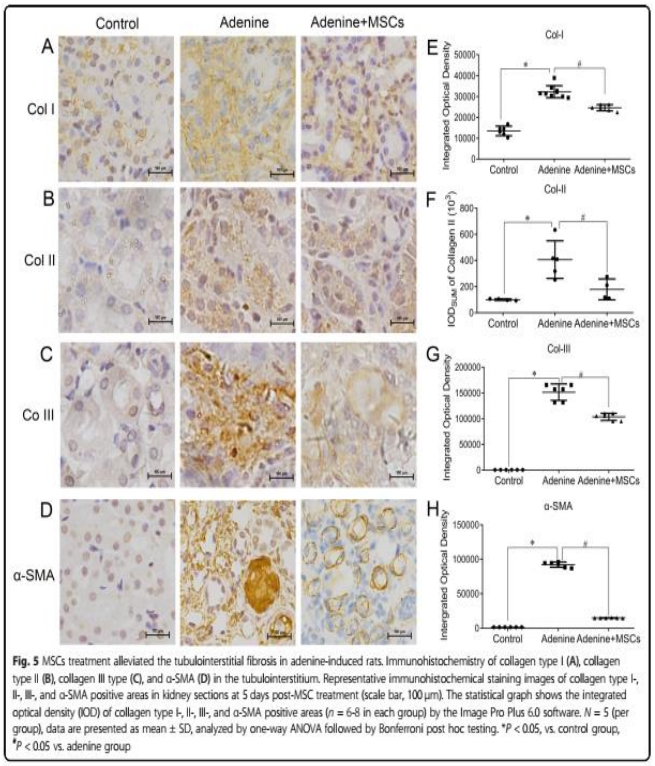

Fig. 5 MSCs treatment alleviated the tubulointerstitial fibrosis in adenine-induced rats. Immunohistochemistry of collagen type I **(A)**, collagen type II **(B)**, collagen III type **(C)**, and α-SMA **(D)** in the tubulointerstitium. Representative immunohistochemical staining images of collagen type I-, II-, III-, and α-SMA positive areas in kidney sections at 5 days post-MSC treatment (scale bar, 100 μm). The statistical graph shows the integrated optical density (IOD) of collagen type I-, II-, III-, and α-SMA positive areas (n = 6-8 in each group) by the Image Pro Plus 6.0 software. $N = 5$ (per group), data are presented as mean ± SD, analyzed by one-way ANOVA followed by Bonferroni post hoc testing. $^{*}P < 0.05$, vs. control group, $^{\#}P < 0.05$ vs. adenine group

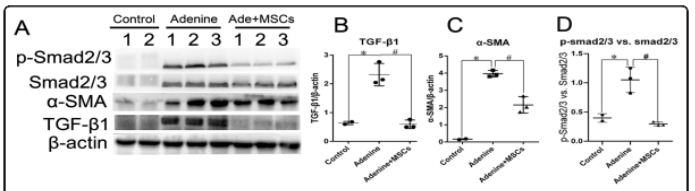

Fig. 6 MSC treatment ameliorated TGF-β1/Smad signaling pathway in adenine-induced rats by western blot analysis of α-SMA, p-Smad2/3, Smad2/3, and TGF-β1 in kidney tissues (**A**). The statistical graph shows the densitometric analysis of TGF-β1 (**B**), α-SMA (**C**), and p-Smad2/3 vs. Smad2/3 (**D**) expression normalized to β-actin expression. All experiments were repeated at least 3 times, and similar results were obtained each time. $N = 3$ (per group), data are presented as mean ± SD, analyzed by one-way ANOVA followed by Bonferroni post hoc testing. $^{*}P < 0.05$, vs. control group. $^{\#}P < 0.05$ vs. adenine group

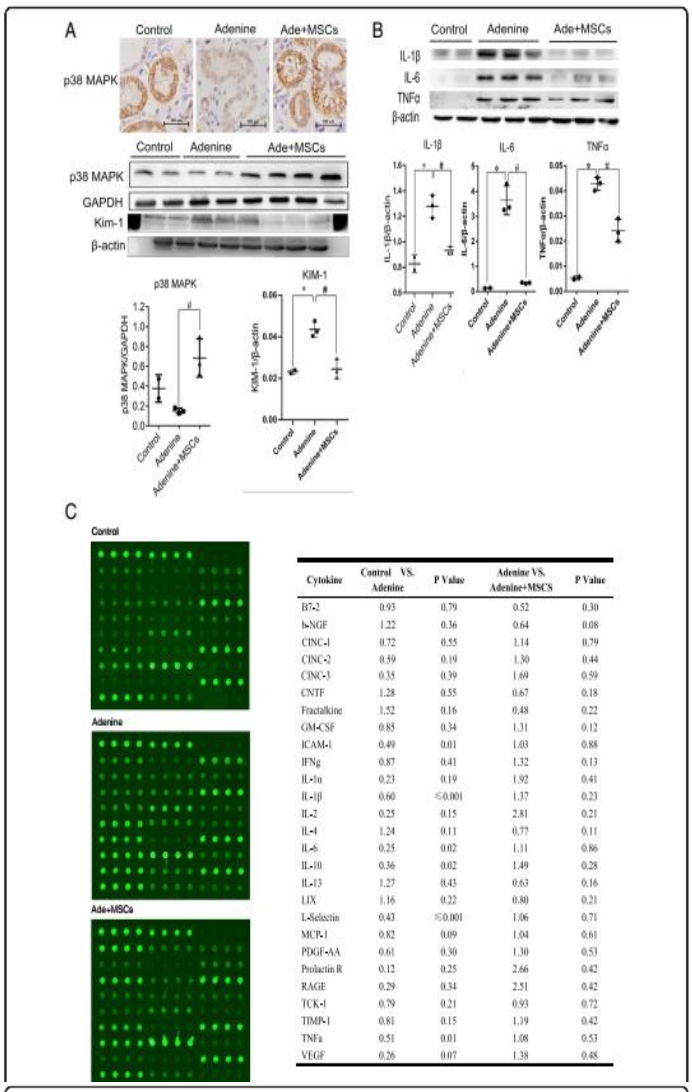

Cytokine	Control VS. Adenine	P Value	Adenine VS. Adenine+MSCS	P Value
B7-2	0.93	0.79	0.52	0.30
b-NGF	1.22	0.36	0.64	0.08
CINC-1	0.72	0.55	1.14	0.79
CINC-2	0.59	0.19	1.30	0.44
CINC-3	0.35	0.39	1.69	0.59
CNTF	1.28	0.55	0.67	0.18
Fractalkine	1.52	0.16	0.48	0.22
GM-CSF	0.85	0.34	1.31	0.12
ICAM-1	0.49	0.01	1.03	0.88
IFNg	0.87	0.41	1.32	0.13
IL-1a	0.23	0.19	1.92	0.41
IL-1β	0.60	≤0.001	1.37	0.23
IL-2	0.25	0.15	2.81	0.21
IL-4	1.24	0.11	0.77	0.11
IL-6	0.25	0.02	1.11	0.86
IL-10	0.36	0.02	1.49	0.28
IL-13	1.27	0.43	0.63	0.16
LIX	1.16	0.22	0.80	0.21
L-Selectin	0.43	≤0.001	1.06	0.71
MCP-1	0.82	0.09	1.04	0.61
PDGF-AA	0.61	0.30	1.30	0.53
Prolactin R	0.12	0.25	2.66	0.42
RAGE	0.29	0.34	2.51	0.42
TCK-1	0.79	0.21	0.93	0.72
TIMP-1	0.81	0.15	1.19	0.42
TNFa	0.51	0.01	1.08	0.53
VEGF	0.26	0.07	1.38	0.48

(See figure on previous page.)
Fig. 7 MSCs activated p38 MAPK signaling and reduced inflammation and kidney injury in adenine-induced rats. **A** Immunohistochemistry and western blot of p38 MAPK and Kim-1 in kidney tissues. **B** Western blot analysis of IL-6, IL-1β, and TNFα in kidney tissue. Representative immunohistochemical staining images in kidney sections (scale bar, 100 μm) and representative western blot images of p38 MAPK protein at 5 days post-MSCs treatment. The statistical graph shows the densitometric analysis of p38 MAPK expression normalized to GAPDH expression, and of Kim-1, IL-6, IL-1β, and TNFα expression normalized to β-actin expression. All experiments were repeated at least 3 times, and similar results were obtained each time. $N = 3$ (per group), data are presented as mean ± SD, analyzed by one-way ANOVA followed by Bonferroni post hoc testing. $^{*}P < 0.05$, vs. control group. $^{\#}P < 0.05$ vs. adenine group. **C** Microarray analysis of cytokine antibodies revealed that a total of 17 cytokines increased in the serum, such as CINC-1, CINC-2, CINC-3, GM-CSF, ICAM-1, IFNγ, IL-1α, IL-2, IL-6, IL-10, L-Selectin, MCP-1, PDGF-AA, Prolactin R, RAGE, TCK-1, TIMP-1, and VEGF, and a total of 8 cytokines decreased, including b-NGF, CNTF, Fractalkine, IL-1β, IL-4, IL-13, LIX, and TNFα in the adenine group. Among them, there were significantly statistical differences in both increases in ICAM-1, IL-10, and L-Selectin and reduction in IL-1β. While MSCs treatment reduced the serum levels of 18 upregulated cytokines and increased the serum levels of 8 downregulated cytokines. $N = 5$ (in each group), the mean value of four replicates was first calculated as the signal value of each factor, then the signal value was normalized to positive control to allow comparison between subarrays, and finally, the concentration was relatively quantified by using the normalized data. The intergroup ratio of 27 factors was calculated, and the P values between groups were analyzed by t TEST (double-tailed)

Table 1 Protein quantitative statistics

Comparisons	Up-	Down-	All-
Adenine vs. control	2027	1029	3056
Adenine+MSCs vs. control	1855	922	2777
Adenine+MSCs vs. adenine	30	10	40
Total	3912	1961	5873

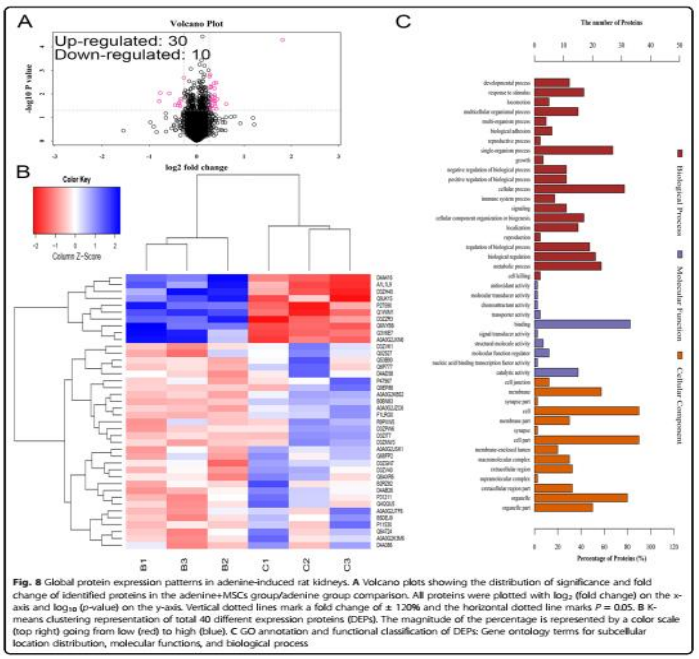

Fig. 8 Global protein expression patterns in adenine-induced rat kidneys. **A** Volcano plots showing the distribution of significance and fold change of identified proteins in the adenine+MSCs group/adenine group comparison. All proteins were plotted with $\log_2$ (fold change) on the x-axis and $\log_{10}$ (p-value) on the y-axis. Vertical dotted lines mark a fold change of ± 1.20% and the horizontal dotted line marks $P = 0.05$. **B** K-means clustering representation of total 40 different expression proteins (DEPs). The magnitude of the percentage is represented by a color scale (top right) going from low (red) to high (blue). **C** GO annotation and functional classification of DEPs: Gene ontology terms for subcellular location distribution, molecular functions, and biological process

Table 2 Differentially expressed proteins between the adenine+MSCs group and the adenine group

Accession	Gene Name	Adenine+MSCs group vs. adenine group ratio	Regulated	*P* value
B0BN83	Armc1	3.52	Up	≤0.001
Q02527	Mgat3	1.54	Up	0.027
Q6AXR6	Gsto1	1.35	Up	0.017
Q9EP88	Slc25a14	1.34	Up	0.043
A0A0G2JZC6	Arhgef11	1.33	Up	0.003
D4AD58	Etfrf1	1.31	Up	0.033
Q6P777	Mvb12a	1.31	Up	0.021
D3ZPW6	Lage3	1.30	Up	0.011
Q64724	LOC103689942	1.30	Up	0.026
D3ZMW3	Msto1	1.30	Up	0.014
B5DEJ9	Sbf2	1.30	Up	0.006
A0A0G2JSK1	Serpina3c	1.29	Up	0.003
Q4QQU5	Yipf6	1.28	Up	0.020
D4A3B6	Cldn2	1.27	Up	0.042
P31211	Serpina6	1.26	Up	0.013
Q68FP2	Pon3	1.26	Up	0.017
Q53B90	Rab43	1.25	Up	0.031
D3ZV40	Unk	1.23	Up	0.005
D4A826	Smc6	1.23	Up	0.005
P11530	Dmd	1.23	Up	0.037
A0A0G2K3M6	Atp9b	1.22	Up	0.017
D3ZGN7	Mical3	1.22	Up	0.011
D3ZVK1	Mcm8	1.22	Up	0.005
F1LRG0	Cyp21a1	1.22	Up	0.001
A0A0G2KB52	Map7	1.21	Up	0.002
B2RZB2	Pcgf2	1.21	Up	0.043
R9PXW5	Nme6	1.20	Up	0.035
A0A0G2JTF6	Thtpa	1.20	Up	0.040
D3ZIT7	LOC103689975	1.20	Up	0.026
P47967	Lgals5	1.20	Up	0.048
Q1WIM1	Cadm4	0.83	Down	0.002
D3ZZR3	Ctss	0.79	Down	0.016
D3ZH40	Otud7b	0.79	Down	0.020
Q9JK15	Adap2	0.79	Down	0.033
G3V6E7	Fmod	0.77	Down	0.024
A1L1L9	Tmem65	0.76	Down	0.030
P27590	Umod	0.73	Down	0.030
D4A416	Clptm1l	0.67	Down	0.010
Q6NYB8	Ifi47	0.59	Down	0.009
A0A0G2JXN6	Galectin-3	0.58	Down	0.020

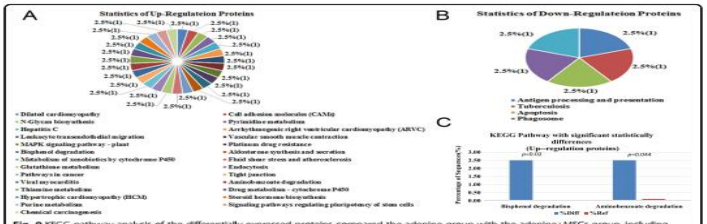

Fig. 9 KEGG pathway analysis of the differentially expressed proteins compared the adenine group with the adenine+MSCs group, including statistics of upregulated proteins (**A**) and statistics of downregulated proteins (**B**). Among these pathways of upregulated proteins, bisphenol degradation and aminobenzoate degradation (**C**) were significantly statistical differences comparing the adenine group with the Adenine+MSCs group. p value was 0.02 and 0.04, respectively

Table 3 List of main KEGG pathways between the adenine group and the Ade+MSCs group

MapName	Number	Upregulated proteins accession (gene name)	*P* value
N-Glycan biosynthesis	1	Q02527 (Mgat3)	0.14
MAPK signaling pathway	1	R9PXW5 (Nme6)	0.07
Bisphenol degradation	1	Q68FP2 (Pon3)	0.02
Aminobenzoate degradation	1	Q68FP2 (Pon3)	0.04
Thiamine metabolism	1	A0A0G2JTF6 (Thtpa)	0.06
Steroid hormone biosynthesis	1	F1LRG0 (Cyp21a1)	0.12
Signaling pathways regulating pluripotency of stem cells	1	B2RZB2 (Pcgf2)	0.17

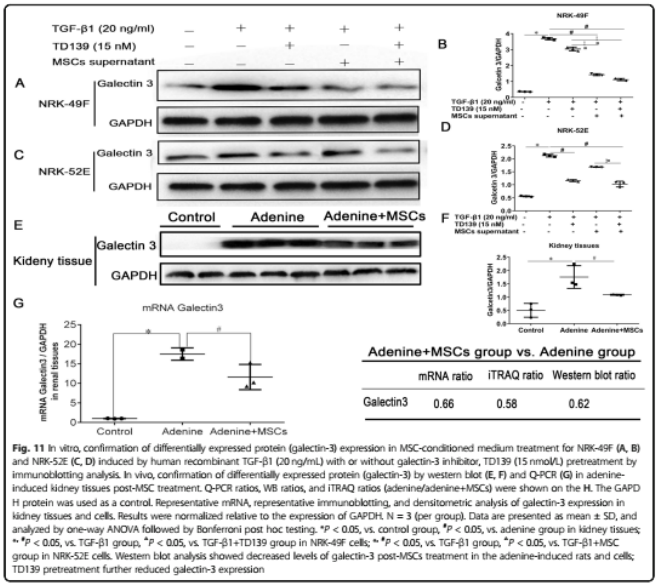

Fig. 11 In vitro, confirmation of differentially expressed protein (galectin-3) expression in MSC-conditioned medium treatment for NRK-49F **(A, B)** and NRK-52E **(C, D)** induced by human recombinant TGF-β1 (20 ng/mL) with or without galectin-3 inhibitor, TD139 (15 nmol/L) pretreatment by immunoblotting analysis. In vivo, confirmation of differentially expressed protein (galectin-3) by western blot **(E, F)** and Q-PCR **(G)** in adenine-induced kidney tissues post-MSC treatment. Q-PCR ratios, WB ratios, and iTRAQ ratios (adenine/adenine+MSCs) were shown on the H. The GAPDH protein was used as a control. Representative mRNA, representative immunoblotting, and densitometric analysis of galectin-3 expression in kidney tissues and cells. Results were normalized relative to the expression of GAPDH. N = 3 (per group). Data are presented as mean ± SD, and analyzed by one-way ANOVA followed by Bonferroni post hoc testing. *$P < 0.05$, vs. control group, $^{\#}P < 0.05$, vs. adenine group in kidney tissues; *, $^{\#}P < 0.05$, vs. TGF-β1 group, *$P < 0.05$, vs. TGF-β1+TD139 group in NRK-49F cells; *, $^{\#}P < 0.05$, vs. TGF-β1 group, *$P < 0.05$, vs. TGF-β1+MSC group in NRK-52E cells. Western blot analysis showed decreased levels of galectin-3 post-MSCs treatment in the adenine-induced rats and cells; TD139 pretreatment further reduced galectin-3 expression

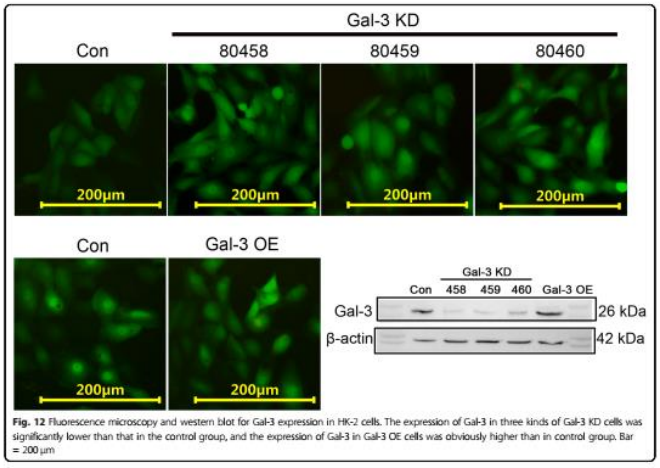

Fig. 12 Fluorescence microscopy and western blot for Gal-3 expression in HK-2 cells. The expression of Gal-3 in three kinds of Gal-3 KD cells was significantly lower than that in the control group, and the expression of Gal-3 in Gal-3 OE cells was obviously higher than in control group. Bar = 200 μm

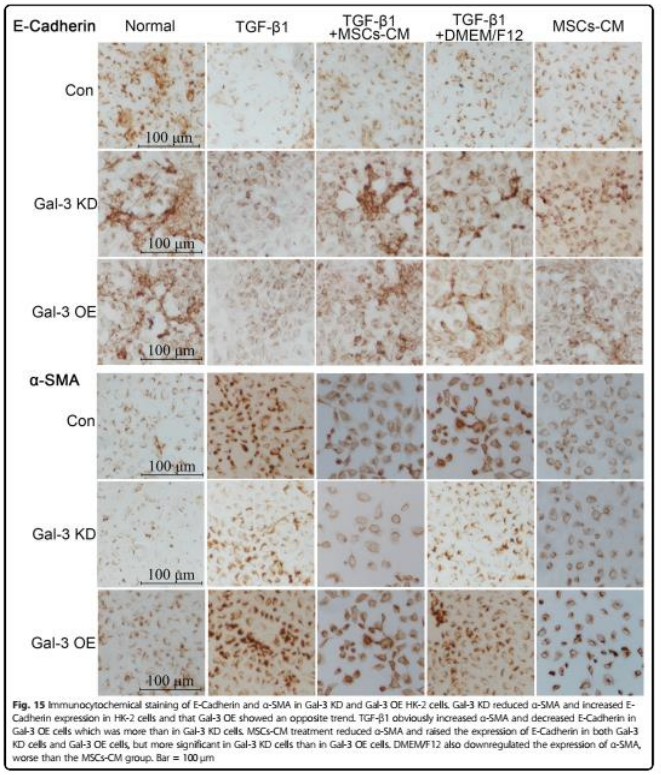

Fig. 15 Immunocytochemical staining of E-Cadherin and α-SMA in Gal-3 KD and Gal-3 OE HK-2 cells. Gal-3 KD reduced α-SMA and increased E-Cadherin expression in HK-2 cells and that Gal-3 OE showed an opposite trend. TGF-β1 obviously increased α-SMA and decreased E-Cadherin in Gal-3 OE cells which was more than in Gal-3 KD cells. MSCs-CM treatment reduced α-SMA and raised the expression of E-Cadherin in both Gal-3 KD cells and Gal-3 OE cells, but more significant in Gal-3 KD cells than in Gal-3 OE cells. DMEM/F12 also downregulated the expression of α-SMA, worse than the MSCs-CM group. Bar = 100 μm

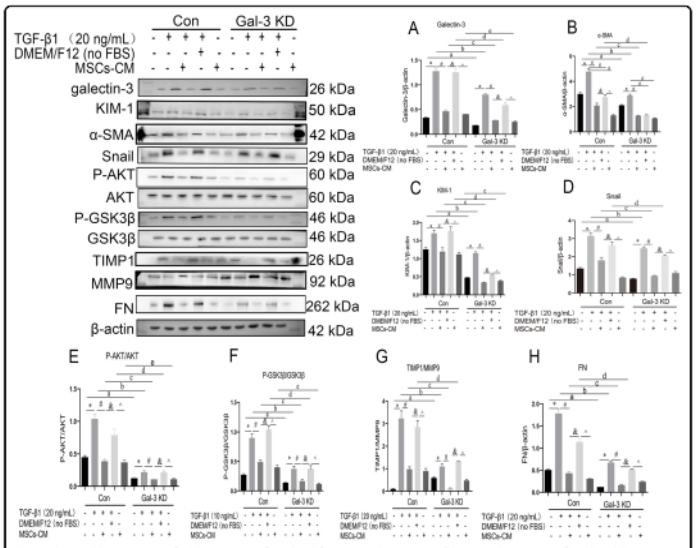

Fig. 13 The possible mechanism of MSCs against TGF-β1-induced fibrosis in Gal-3 KD HK-2 cells. In control groups, TGF-β1 induced the obvious increases in Gal-3 **(A)**, α-SMA **(B)**, KIM-1 **(C)**, Snail **(D)**, p-Akt (Ser473) **(E)**, p-GSK3β (Ser9) **(F)**, the ratio of TIMP1/MMP9 **(G)**, and FN **(H)** compared with the normal group. MSCs-CM treatment notably decreased the expressions of above indexes after TGF-β1 treatment or only MSCs-CM without TGF-β1 treatment. DMEM/F12 medium treatment with no serum significantly upregulated these indexes compared with the TGF-β1+MSCs-CM group, especially the expression of KIM-1 and the ratio of p-GSK3β/GSK3β more than TGF-β1 group. In Gal-3 KD groups, the trends of each group were similar to those of the control groups, but lower than the same subgroup in control cells. DMEM/F12 treatment also resulted in obvious increases of aforementioned indexes compared with the TGF-β1+MSCs-CM group, but the expression of KIM-1 lower than the TGF-β1 group, and the ratio of p-GSK3β/GSK3β close to the TGF-β1 group. Results were normalized relative to the expression of β-actin. N = 3 (per group). Data are presented as mean ± SD, and analyzed by two-way ANOVA followed by Tukey post hoc testing. *$P < 0.05$, vs. control group, $^{\#}P < 0.05$, vs. TGF-β1+MSCs-CM group, $^{\&}P < 0.05$, vs. TGF-β1 +DMEM/F12 group, $^{\wedge}P < 0.05$, vs. MSCs-CM group; compared empty transfection HK-2 cells with Gal-3 KD HK-2 cells, $^{a}P < 0.05$, vs. normal group, $^{b}P < 0.05$, vs. TGF-β1 group , $^{c}P < 0.05$, vs. TGF-β1+MSCs -CM group, $^{d}P < 0.05$, vs. TGF-β1+MSCs-CM group, $^{e}P < 0.05$, vs. MSCs-CM group

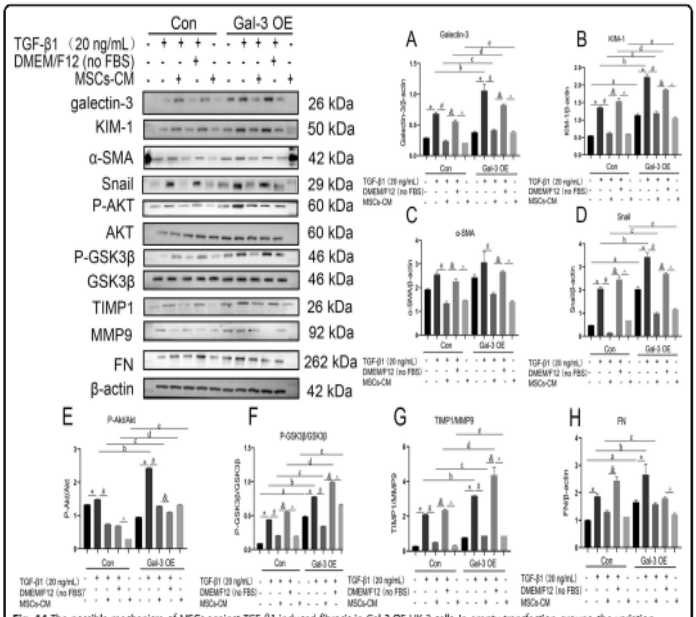

Fig. 14 The possible mechanism of MSCs against TGF-β1 induced fibrosis in Gal-3 OE HK-2 cells. In empty transfection groups, the variation trends **(A–H)** of each group were similar to Fig. 13. In Gal-3 OE groups, the variation trends of each group were similar to those of the control groups and Gal-3 KD groups, but higher than the same subgroup in Gal-3 KD cells. In TGF-β1+DMEM/12 group, the expression of KIM-1 was also lower than TGF-β1 group, but the ratios of p-GSK3β/GSK3β and TIM1P1/MMP9 were higher than TGF-β1 group. Results were normalized relative to the expression of β-actin. *N* = 3 (per group). Data are presented as mean ± SD, and analyzed by two-way ANOVA followed by Tukey post hoc testing. *$P < 0.05$, vs. control group, $^{\#}P < 0.05$, vs. TGF-β1+MSCs-CM group, $^{\&}P < 0.05$, vs. TGF-β1 +DMEM/F12 group, $^{\wedge}P < 0.05$, vs. MSCs-CM group; compared empty transfection HK-2 cells with Gal-3 KD HK-2 cells, $^{a}P < 0.05$, vs. normal group, $^{b}P < 0.05$, vs. TGF-β1 group , $^{c}P < 0.05$, vs. TGF-β1+MSCs -CM group, $^{d}P < 0.05$, vs. TGF-β1+MSCs-CM group, $^{e}P < 0.05$, vs. MSCs-CM group

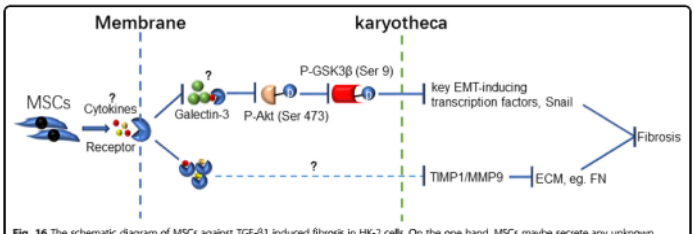

Fig. 16 The schematic diagram of MSCs against TGF-β1 induced fibrosis in HK-2 cells. On the one hand, MSCs maybe secrete any unknown cytokines which enter the cytoplasm through receptors, somehow bind to galectin-3, and inhibit phosphorylation of Akt (Ser473) and GSK3β (Ser9), next inhibiting downstream key EMT-inducing transcription factors, Snail. On the other hand, MSCs probably balance the ratio of TIMP1/MMP9 which regulates ECM generation and degradation. Ultimately, MSCs alleviate TGF-β1-inducing fibrosis in HK-2 cells. Further research is needed to explore which concrete cytokine secreted by MSCs interacts with galectin-3 and how to regulate the balance of TIMP1/MMP9

Recent Publications (minimum 5)

1. Vazquez-Mendez E, Gutierrez-Mercado Y, Mendieta-Condado E, GalvezGastelum FJ, Esquivel-Solis H, Sanchez-Toscano Y, et al. Recombinant erythropoietin provides protection against renal fibrosis in adenine-induced chronic kidney disease. Mediators Inflamm. 2020;2020:8937657.
2. Tomita T, Goto H, Sumiya K, Yoshida T, Tanaka K, Kohda Y. Efficacy of adenine in the treatment of leukopenia and neutropenia associated with an overdose of antipsychotics or discontinuation of lithium carbonate administration: three case studies. Clin Psychopharmacol Neurosci. 2016;14(4):391–5.
3. Boon AC, Lam AK, Gopalan V, Benzie IF, Briskey D, Coombes JS, et al. Endogenously elevated bilirubin modulates kidney function and protects from circulating oxidative stress in a rat model of adenine-induced kidney failure. Sci Rep. 2015;5(1):15482.
4. El Agha E, Kramann R, Schneider RK, Li X, Seeger W, Humphreys BD, et al. Mesenchymal stem cells in fibrotic disease. Cell Stem Cell. 2017;21(2):166–77.
5. Fitzsimmons REB, Mazurek MS, Soos A, Simmons CA. Mesenchymal stromal/ stem cells in regenerative medicine and tissue engineering. Stem Cells Int. 2018;2018:8031718.
6. Yokote S, Katsuoka Y, Yamada A, Ohkido I, Yokoo T. Effect of adiposederived mesenchymal stem cell transplantation on vascular calcification in rats with adenine-induced kidney disease. Sci Rep. 2017;7(1):14036.
7. Anan HH, Zidan RA, Shaheen MA, Abd-El Fattah EA. Therapeutic efficacy of bone marrow derived mesenchymal stromal cells versus losartan on adriamycin-induced renal cortical injury in adult albino rats. Cytotherapy. 2016;18(8):970–84.
8. Moghadasali R, Azarnia M, Hajinasrollah M, Arghani H, Nassiri SM, Molazem M, et al. Intra-renal arterial injection of autologous bone marrow mesenchymal stromal cells ameliorates cisplatin-induced acute kidney injury in a rhesus Macaque mulatta monkey model. Cytotherapy. 2014;16(6):734–
9. Cao H, Cheng Y, Gao H, Zhuang J, Zhang W, Bian Q, et al. In vivo tracking of mesenchymal stem cell-derived extracellular vesicles improving mitochondrial function in renal ischemia-reperfusion injury. ACS Nano. 2020; 14(4):4014–26.

西南医科大學
SOUTHWEST MEDICAL UNIVERSITY

Biography (150 word limit)

Dr. Bo Chen, deputy director of Department of Human Anatomy and Embryology, comes from School of Basic Medical Sciences, Southwest Medical University, Luzhou city, Sichuan Province, China. He has his expertise in stem cells treatment for acute or chronic kidney diseases. He devotes to exploring the new mechanism of renal fibrosis in MSCs against renal fibrosis, and looking for the effective anti-fibrotic targets and drugs.

Email: mailto:cb0402022@semu.edu.cn

Notes/Comments:

Presenting author details

Full name: Bo Chen
Contact number: +8618980258613
Mail id: cb0402022@swmu.edu.cn

Category: (Oral presentation/ Poster presentation) Online communication and Poster presentation